ISIJ International, Vol. 54 (2014), No. 6, pp. 1283–1287

Influence of a Slow Rotating Magnetic Field in Thermoelectric Magnetohydrodynamic Processing of Alloys

Andrew KAO,[1)]* Peter David LEE[2)] and Koulis PERICLEOUS[1)]

1) Centre for Numerical Modelling and Processes Analysis, University of Greenwich, Old Royal Naval College, Park Row, London, SE10 9LS.
2) The Manchester X-Ray Imaging Facility, School of Materials, The University of Manchester, Oxford Rd., M13 9PL, UK.

(*Received on September 5, 2013; accepted on January 29, 2014*)

The effects of a slow rotating magnetic field on Thermoelectric Magnetohydrodynamics during alloy solidification were investigated using a micro-scale numerical model. For conventional directional solidification it was shown that in general the time-dependent acceleration force on the fluid flow is negligible. Using an undercooled growth model with directional solidification approximations the effect on dendritic morphology is predicted, suggesting thermoelectric induced flows will create a significant increase in secondary branching and preferential growth directions on one side of the primary trunk. The extent of macro-segregation under these conditions was also estimated.

KEY WORDS: Thermoelectric Magnetohydrodynamics; rotating magnetic field; directional solidification.

1. Introduction

During alloy solidification, thermoelectric currents form due to temperature variations along the liquid-solid interface. In the presence of an external magnetic field these currents interact to form a Lorentz force, driving fluid motion in the liquid. This phenomenon is known as Thermoelectric Magnetohydrodynamics (TEMHD) and experimental results for both high[1)] and low[2)] magnetic fields have shown that the application of a constant external magnetic field can cause fragmentation, acting to produce a finer grained casting, with a concomitant increase in yield strength. However, the undesirable effect of macro-segregation[3–5)] and freckling[6)] have been observed. Both of these effects can be attributed to the convective transport of heat and mass, altering the solidification process. The effect of convective transport is highly dependent on all aspects of the magnetic field including, orientation,[7)] magnitude and time dependent fluctuations.[8)] Grain refinement has been observed through the use of pulsed magnetic fields.[9,10)] A slow rotating magnetic field has been shown to produce a helical structure,[11)] which can be attributed to a modification in convective segregation. This paper investigates the possibility of using a slow rotating magnetic field to retain the effect of grain refinement while mitigating macro-segregation. Developing such a technique could be massively beneficial to a wide range of applications. This includes traditional systems such as continuous casting,[12)] where the thermal conditions are analogous to directional solidification. In more complex systems such as the Vacuum Arc Remelting,[13)] an external current is already present that could be manipulated in a similar fashion to thermoelectric currents. Coupling TEMHD to existing mechanisms could provide a novel method for further mitigating unwanted effects, for example the formation of freckles.[14)] The effect of TEMHD on dendritic morphology has been observed with magnetic fields lower than 1 T and within the range of permanent magnets. This numerical analysis focuses entirely on the underlying transport mechanism of TEMHD under a slow rotating field. The predicted morphological changes show that grain refinement can be achieved. By increasing knowledge of this phenomenon could provide another soldification tool (alongside traditional methods) for tailoring the microstructure. For many applications this could provide the added thermophyisical benefits for a relatively low cost of implementation.

2. Modelling Approach

The fundamentals of TEMHD were derived by Shercliff,[15)] where Ohm's law was generalised to include an extra term accounting for thermoelectric currents:

$$\frac{\mathbf{J}}{\sigma} = \mathbf{E} - S\nabla T + \mathbf{u}\times\mathbf{B} \quad \text{..... (1)}$$

where S is the Seebeck coefficient and T the temperature. Interaction with the magnetic field gives the Lorentz force, which appears as a body force in the incompressible Navier-Stokes Eq. (2). The final term in (2) is a Darcy resistance term that prevents flow in solid regions, where f is the liquid fraction and η is the permeability:

$$\rho\frac{d\mathbf{u}}{dt} + \rho\mathbf{u}\cdot\nabla\mathbf{u} = -\nabla p + \mu\nabla^2\mathbf{u} + \mathbf{J}\times\mathbf{B} - \left(\frac{1-f^2}{f^3}\right)\frac{\mu\mathbf{u}}{\eta} \quad \text{... (2)}$$

* Corresponding author: E-mail: a.kao@gre.ac.uk
DOI: http://dx.doi.org/10.2355/isijinternational.54.1283

In this work solidification is modelled using an Enthalpy based method.[16] The volumetric enthalpy H is defined as the sum of sensible latent heats:

$$H = c_p T + fL \quad \text{..... (3)}$$

where c_p is the volumetric specific heat capacity and L is the volumetric latent heat of fusion. For binary alloys the concentration potential V in terms of the solute concentration C and partitioning coefficient k is defined as:[17]

$$V = \frac{C}{f(1-k)+k} \quad \text{..... (4)}$$

The interfacial temperature (T^i) is given by the Gibbs-Thompson condition:

$$T^i = T_m - \frac{\gamma(\theta,\phi)}{L} T_m \kappa - m\left(C_0 - C_l^i\right) \quad \text{..... (5)}$$

where T_m is the melting temperature, $\gamma(\theta, \phi)$ is the surface energy, κ the curvature, m the liquidus slope, C_0 the bulk solute concentration and C_l^i the liquid solute concentration at the interface. Finally transport of heat and mass are given by:

$$\frac{dH}{dt} = \nabla\cdot\left(K\nabla T\right) - \nabla\cdot\left(\mathbf{u}H\right) \quad \text{..... (6)}$$

$$\frac{dC}{dt} = \nabla\cdot\left(D_l\nabla V\right) - \nabla\cdot\left(\mathbf{u}C\right) \quad \text{..... (7)}$$

where K is the thermal conductivity and D_l is the liquid mass diffusivity. Contrary to traditional applications of rotating magnetic fields, the angular frequency in this study is considered to be sufficiently low (order of seconds) that the effect of induced currents from the rotation are negligible. Consequently the Lorentz force is considered to be comprised of only the interaction between the thermoelectric currents and electromagnetic damping.

For numerical stability all of the equations are solved in a dimensionless form. All dimensionless terms are represented by the superscript *. Characteristic scaling factors are obtained for the base SI units and take the form given in **Table 1**, where α is the thermal diffusivity.

A consequence of scaling in this way sets $\rho^* = \sigma^* = \alpha^* = 1$.[18] **Table 2** provides typical thermophysical properties for an Al system that will be used throughout this paper unless otherwise specified.

The fully coupled transient undercooled numerical model incorporates three distinct solution steps: 1. for a given state of the system the thermoelectric currents are solved, 2. the corresponding Lorentz force is then used to solve for velocity, and 3. the velocities are then used to update the thermal and solute fields and finally the liquid-solid interface is updated based on the change to local free energy. A more detailed description of the fully coupled model, formulation of the key equations, discretisation and numerical implementation is given by Kao and Pericleous.[18,19] Directly coupling directional solidification with TEMHD is currently beyond the scope of this study due to computational limitations. There is a large disparity in the characteristic time scales between undercooled growth and directional solidification, it is therefore necessary to calculate significantly larger number of time steps to observe a similar effect. This is currently being addressed by converting the code to run in parallel on GPUs and examining stability and convergence criteria of the Enthalpy method in directional solidification. Therefore, to gain an insight into the effect a rotating magnetic field, the approximations detailed above were implemented in the current sequential code, allowing for a quasi-representation of directional solidification.

3. Fluid Flow under a Rotating Magnetic Field

By decoupling solidification from the fluid flow it is possible to gain an understanding of how the fluid behaves under a rotating field. For this case the effects of heat and mass transport are neglected, for diffusion it is assumed that the dendrite is in thermodynamic equilibrium and for convection it is assumed that the velocity is low. The latter could be achieved through a low Seebeck power. Under these assumptions the dendrite morphology remains constant. The surface temperature of the dendrite is assumed to vary linearly along the direction of the thermal gradient; allowing for a time-independent solution for the thermoelectric currents. To give a reasonable representation of the morphology the dendrite was grown from undercooled conditions of $\Delta T^* = -0.5$; providing a relatively fine grain size (50 μm) and has some similarities to directional solidification under a high thermal gradient. **Figure 1** shows the morphology, the corresponding thermoelectric currents and an indication of the orientation of the magnetic field through one quarter rotation about the z axis. Assuming an infinitesimally small Seebeck power, then only the direction of J and relative magnitude is required to examine the fluid behaviour.

A 1.2 T transverse (orthogonal to ∇T) rotating magnetic

Table 1. Scaling factors for dimensionless system.

Base SI Unit	Scaling Factor
Temperature (K)	$T_0 = \frac{L}{c_p}$
Length (m)	$x_0 = \left(\alpha t_0\right)^{1/2}$
Time (s)	$t_0 = \frac{\alpha}{L}$
Mass (Kg)	$m_0 = \rho x_0^3$
Current (A)	$A_0 = \left(\frac{m_0 x_0^3 \sigma}{t_0^3}\right)^{1/2}$

Table 2. Typical thermophysical properties for an Al system.

Property	Variable	Typical Value	Units
Density	ρ	2.3×10^3	Kg/m^3
Dynamic viscosity	μ	1.3×10^{-3}	Pas
Electrical conductivity	σ	3.78×10^7	S/m
Thermoelectric field	$S\nabla T$	1×10^{-3}	V/m
Magnetic flux density	B	1.2	T
Characteristic velocity	u	0.35	mm/s
Characteristic time	Δt	1	s
Characteristic length	Δx	5	μm

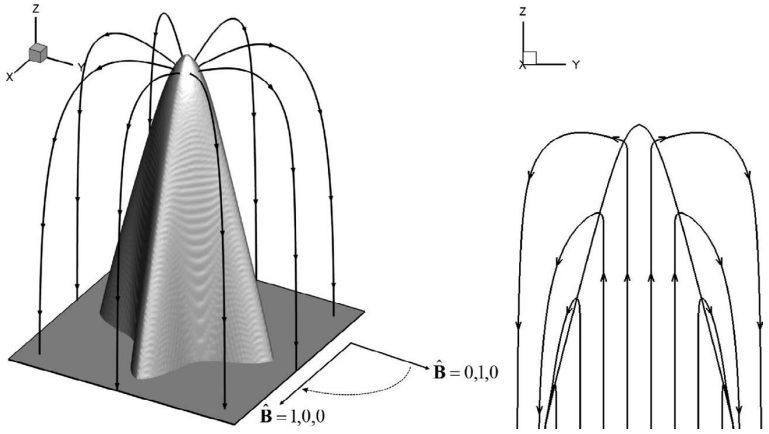

Fig. 1. Morphology and thermoelectric currents in directional solidification: The dendrite is grown from undercooled conditions ($\Delta T^* = -0.5$), while the thermoelectric currents are solved by assuming a linear thermal field on this morphology.

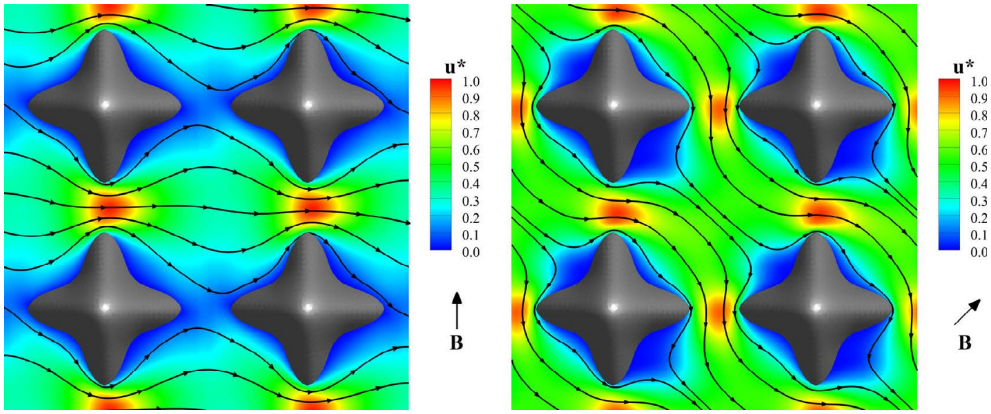

Fig. 2. Time dependent velocity during the rotation of the magnetic field. Left: t = 1 s ($\hat{\mathbf{B}}$ = 1,0,0). Right: t = 1.125 s ($\hat{\mathbf{B}}$ = 1,1,0). (Online version in color.)

field is imposed with a rotational period of 1 s. **Figure 2** shows the normalised velocity field (**u***) at t = 1 s ($\hat{\mathbf{B}}$ = 0,1,0) and t = 1.125 s ($\hat{\mathbf{B}}$ = 1,1,0). Comparing these two solutions to steady state at the corresponding orientation of the magnetic field gives almost identical velocity fields. Thus under these conditions, for rotational periods of the order of 1 s and greater the transient acceleration of the system is negligible and Navier-Stokes can be solved as a series of steady state solutions.

It is also possible to show this behaviour by approximating the governing force equations. Typical thermophysical property values for an Al system are given in Table 2. The characteristic time is defined as the rotational period of the magnetic field (Δt = 1 s) and the characteristic length as the viscous boundary layer (Δx = 5 μm).

Table 3 shows the relative characteristic forces and the approximations for each term in Navier-Stokes equation. From this table it is clear that the time-dependent acceleration force is several orders of magnitude smaller than the other terms.

To achieve a comparable time-dependent acceleration force the frequency of the rotating field would need to be of the order of 10 KHz, however, under this condition many of the approximations taken would no longer be applicable, as the electromagnetic induction would need to be considered. Taking a one dimensional approximation to the Navier-Stokes equation and assuming Re << 1, such that the convective acceleration term can be neglected gives:

$$\rho\frac{du}{dt} = -\sigma S\nabla T + \mu\frac{u}{\Delta x^2} + \sigma uB^2 \quad \text{..... (8)}$$

For an initially stagnant fluid u(t = 0) = 0, the solution for u becomes:

$$u = \frac{\sigma S\nabla TB}{\left(\frac{\mu}{\Delta x^2} + \sigma B^2\right)}\left(1 - e^{-\left(\frac{\mu}{\Delta x^2}+\sigma B^2\right)t/\rho}\right) \quad \text{..... (9)}$$

Figure 3 shows the acceleration time, where a steady state flow (u_{ss}) is achieved in approximately 150 μs, which is much smaller than the rotation periods under consideration. Interestingly this time is comparable to the rotational period required for the time-dependent acceleration to be comparable to the other forces.

4. Solidification under a Rotating Magnetic Field

In this section an undercooled solidification model with approximations to represent directional solidification is used to give an insight into the changes that occur to the dendritic morphology. The first approximation is to decouple the flow solver. In the previous section, it was shown that for direc-

tional solidification under a slowly rotating magnetic field the time-dependent acceleration can be neglected, allowing the Navier-Stokes equation to be solved as a series of steady state solutions. The second approximation is to neglect electromagnetic induction due to the rotating field as the frequency is of the order of 1 Hz. However, due to the much larger growth velocities observed in undercooled growth (of the order of 10 m/s), it is necessary to 'tune' the magnetic field to a much higher frequency and strength otherwise the relative effect would be analogous to a constant magnetic field. Physically this represents unrealistic values of a 5 T field with a frequency of MHz and so it is unlikely that a slow rotating field will have any applications in high undercooled solidification. In undercooled growth TE currents are governed by localised surface temperature variations, while in directional solidification they are predominantly controlled by the external thermal gradient. To represent TE currents in directional solidification using an undercooled model, a fixed high thermoelectric potential under a high thermal gradient is imposed and the surface temperature contributions are neglected. The thermoelectric field $S\nabla T = 7.0\times10^2$ V/m is higher than may be experimentally achievable, but has again been tuned to simulate a representative Péclet number in directional solidification. Consequently the flow velocity is comparable to the tip velocity. **Figure 4** shows the change to morphology and the extent of macro-segregation over one and half clockwise revolutions of the magnetic field.

Table 3. Relative characteristic forces.

Force	Equation	Characteristic Value (N/m^3)
Thermoelectric force	$S\nabla T \times \mathbf{B} \approx \sigma S \nabla T B$	4.5×10^4
Viscous damping	$\mu\nabla^2\mathbf{u} \approx \mu\frac{u}{\Delta x^2}$	1.8×10^4
Electromagnetic damping	$\sigma\mathbf{u}\times\mathbf{B}\times\mathbf{B} \approx \sigma u B^2$	1.9×10^4
Convective acceleration	$\rho\mathbf{u}\cdot\nabla\mathbf{u} \approx \rho\frac{u^2}{\Delta x}$	5.8×10^1
Time-dependent acceleration	$\rho\frac{d\mathbf{u}}{dt} \approx \rho\frac{u}{\Delta t}$	0.83

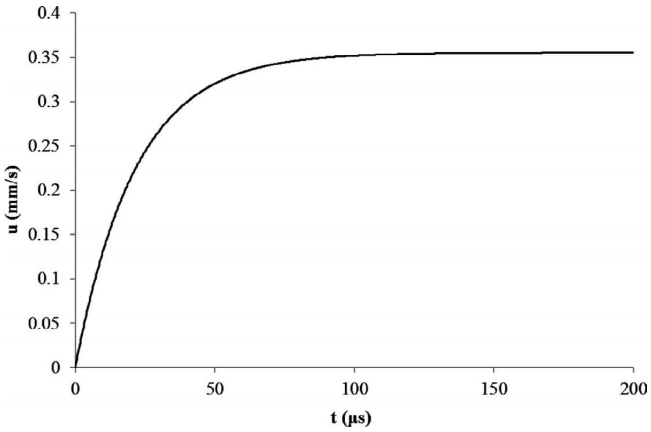

Fig. 3. 1 D analytic estimation of the acceleration time.

The morphological changes due to the rotating field are significant and include an increase in secondary branching with preferential growth on the clockwise side of the branches. These changes are caused by incident flow perturbing the heat and mass boundary layers close to the interface and encouraging growth, while downstream plumes of high solute concentration hot liquid supress growth. As the magnetic field rotates the change in velocity causes these plumes to be pushed back toward the dendrite, the net effect is rotating thermal and solute fields. The maximum velocity is located in the same relative location along the dendrite to the tip. Therefore as the dendrite grows bulk material is introduced into the rotating thermal and solute fields, otherwise one might expect any growth to then re-melt half a rotation later. In the context of macro segregation, the extent of this plume will depend on the rotational period of the heat and solute fields as well as the magnetic field. For very large rotational periods, the system becomes analogous to a con-

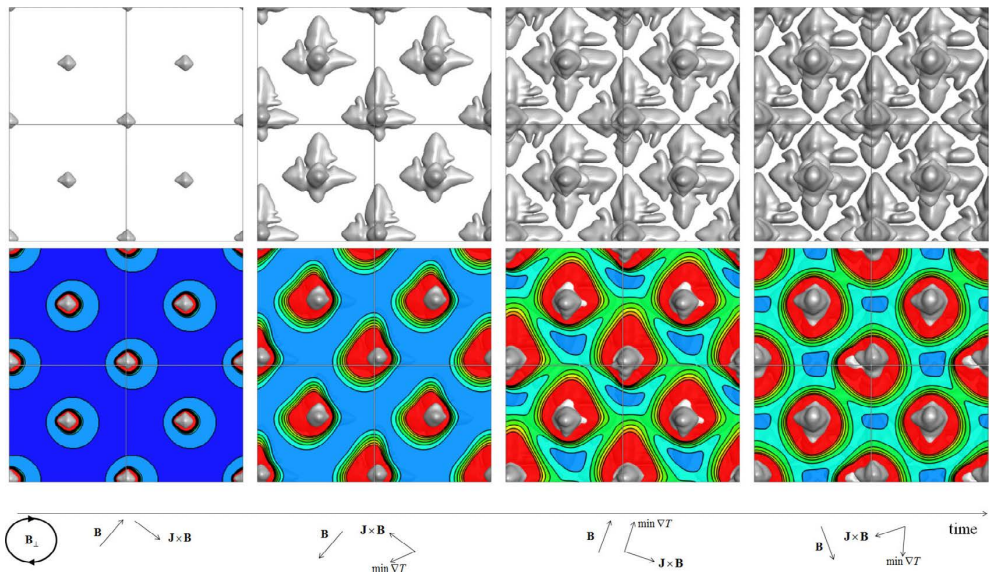

Fig. 4. Solidification coupled to TEMHD. Top: Transient morphology. Bottom: Thermal field scaled to highlight the direction of hot plumes (red indicates hot liquid). The planes chosen have the same relative position of the tip parallel to **J**. The axis indicates the relative direction of the Lorentz force and the direction of plume, min ∇T (omitted in first frame). (Online version in color.)

stant magnetic field, where macro-segregation can cause complete separation of a sample. For relatively smaller rotational periods (still much larger than 150 μs), the flow will accelerate to its maximum and the extent of macro-segregation will depend on the characteristic transport time. A simple approximation is to assume that the force on a fluid particle is sinusoidal over the period of a rotation. The mean velocity over half a rotational period is u_{ss}/π and the macro-segregation distance (λ_r) over this time will be:

$$\lambda_r = \frac{u_{ss}\Delta t}{2\pi} \quad \text{..... (10)}$$

Using typical values from Table 1, this gives $\lambda_r \approx 60$ μm. A more appropriate measurement is to relate λ_r to the grain size, λ_1 (primary arm spacing). The grain size is predominantly given by the external thermal conditions. However, modification of the thermal gradient also plays an important role in determining the magnitude of TEMHD flow. Using the result from Eq. (10) and by simplifying the LKT model to approximate the primary arm spacing,[19] it is possible to approximate the ratio of the macro-segregation distance and the primary arm spacing (grain size) as:

$$\frac{\lambda_r}{\lambda_1} = -\frac{\sigma SB\left(\nabla T\right)^{3/2}\Delta t}{\left(\upsilon^*\right)^{-1/4}\left(\frac{\mu}{\Delta x^2}+\sigma B^2\right)\left(\frac{1152\pi^6\Gamma_{sl}D_l\Delta T_0}{k}\right)^{1/4}} \quad \text{... (11)}$$

where υ^* is the tip velocity, Γ_{sl} the Gibbs-Thompson coefficient and ΔT_0 the equilibrium freezing range. Under fixed electromagnetic conditions all of the terms in this equation are constant except for ∇T and Δt leading to:

$$\frac{\lambda_r}{\lambda_1} \propto \left(\nabla T\right)^{3/2}\Delta t \quad \text{..... (12)}$$

As the thermal gradient increases, so must the rotational period to have an equivalent effect. This trend forms the hypothetical prediction from this work. However, the LKT model does not consider the effects of convection on grain size and it is still unclear as to the effect of TEMHD on grain size irrespective of a rotating magnet. Therefore it is anticipated that this is more applicable to systems of lower velocity through a low/high magnetic field or a low Seebeck power.

5. Conclusions

The effects of TEMHD with a slow rotating magnetic field on alloy solidification have been investigated using a micro-scale numerical model. For conventional directional solidification systems it was shown that in general the time-dependent acceleration force on the fluid flow is negligible in comparison to the driving thermoelectric force, viscous damping and electromagnetic damping. Consequently, for a fixed morphology, the steady state solution of Navier-Stokes equation is almost identical to the transient solution at the same orientation of the magnetic field. By approximating the thermoelectric currents observed in directional solidification to undercooled growth and solving the fluid flow as a series of steady state solutions the effect on dendritic morphology is predicted. The predict impact on dendritic structure is very significant, exhibiting an increase in secondary branching and preferential growth on one side of the primary trunk. Convective transport causes a downstream hot solute rich plume to form, however as the magnet rotates the net macro-segregation of the heat and mass fields also becomes rotational. Using various 1 D analytic solutions and approximations, the extent of macro-segregation is estimated and is related to the grain size.

Acknowledgements

The authors would like to acknowledge the EPSRC (EP/K011413/1, EP/K007734/1) for funding and PDL thanks the Research Complex at Harwell for financial, materials and facilities support (EP/I02249X/1).

REFERENCES

1) X. Li, Y. Fautrelle and Z. Ren: *Acta Mater.*, **55** (2007), 1377.
2) X. Li, Y. Fautrelle and Z. Ren: *Acta Mater.*, **55** (2007), 3803.
3) X. Li, Z. Ren, A. Gagnoud, O. Budebkova and Y. Fautrelle: *Metall. Trans. A*, **42** (2011), 11, 3459.
4) J. Wang, Z. Ren, Y. Fautrelle, X. Li, H. Nguyen-Thi, N. Mangelinck-Noel, G. Salloum Abou Jaoude, Y. Zhong, I. Kaldre and A. Bojarevics: *J. Mater. Sci.*, **48** (2013), 1, 213.
5) I. Kaldre, Y. Fautrelle, J. Etay, A. Bojarevics and L. Buligins: *J. Alloys Compd.*, **571** (2013), 50.
6) R. Moreau, O. Laskar, M. Tanaka and D. Camel: *Mater. Sci. Eng. A*, **173** (1993), 1, 93.
7) A. Kao and K. Pericleous: *J. Iron Steel Int.*, **19** (2012), S1-1, 260.
8) L. Zhang: *Metall. Trans. B*, **44B** (2013), 390.
9) J. W. Fu and Y. S. Yang: *Mater. Lett.*, **67** (2012), 252.
10) Y. J. Li, W. Z. Tao and Y. S. Yang: *J. Mater. Process. Technol.*, **212** (2012), 903.
11) I. Kaldre, Y. Fautrelle, J. Etay and A. Bojarevics: *J. Iron Steel Int.*, **19** (2012), S1-1, 373.
12) P. D. Lee, P. E. Ramirez-Lopez, K. C. Mills and B. Santillana: *Ironmaking Steelmaking*, **39** (2012), No. 4, 244.
13) K. Pericleous, G. Djambazov, M. Ward, L. Yuan and P. D. Lee: *Metall. Trans. A*, **44A** (2013), 5365.
14) L. Yuan and P. D. Lee: *Acta Mater.*, **60** (2012), No. 12, 4917.
15) J. A. Shercliff: *J. Fluid Mech.*, **91** (1979), No. 2, 231.
16) V. R. Voller: *Int. J. Heat Mass Transf.*, **51** (2007), 823.
17) A. Crowley and J. Ockendon: *Int. J. Heat Mass Transf.*, **22** (1979), 941.
18) A. Kao and K. Pericleous: *J. Algorithm. Comput. Tech.*, **6** (2012), No. 1, 50.
19) A. Kao and K. Pericleous: *Magnetohydrodynamics*, **48** (2012), No. 2, 361.
20) J. A. Dantzig and M. Rappaz: Solidification, 1st ed., EFPL Press, Lausanne, France, (2009).